

Mantle flow and olivine fabric transition in the Myanmar continental subduction zone

Enbo Fan^{1,2}, Yinshuang Ai^{1,3,4,*}, Stephen S. Gao^{2,*}, Yumei He^{1,3}, Kelly H. Liu², Mingming Jiang^{1,3,4}, Guangbing Hou¹, Shun Yang¹, Chit Thet Mon¹, Myo Thant⁵, and Kyaing Sein⁶

¹Key Laboratory of Earth and Planetary Physics, Institute of Geology and Geophysics, Chinese Academy of Sciences, 100029 Beijing, China

²Geology and Geophysics Program, Missouri University of Science and Technology, Rolla, Missouri 65409, USA

³Innovation Academy for Earth Science, Chinese Academy of Sciences, 100029 Beijing, China

⁴College of Earth and Planetary Sciences, University of Chinese Academy of Sciences, 100049 Beijing, China

⁵Department of Geology, University of Yangon, 11041 Yangon, Myanmar

⁶Myanmar Geosciences Society, 11051 Yangon, Myanmar

ABSTRACT

One of the major advances in mineral physics and seismology is the realization that different olivine fabric types are functions of temperature, shear stress, and water content in oceanic subducting systems. The distribution of different olivine fabric types and geodynamic processes in the mantle wedge above a subducting continental slab remain poorly understood. Here, based on splitting analysis of shear waves recorded by 46 stations recently deployed in central Myanmar, we reveal trench-perpendicular fast orientations between the 80 and 100 km slab contours sandwiched between trench-parallel fast orientations from the mantle wedge tip to the backarc. The dramatic change in fast orientations indicates the transition of olivine fabric types in the mantle wedge combined with corner flow. Cold continental subduction and shear stress reduction caused by partial melting favor B-type and C- or E-type olivine fabrics, respectively.

INTRODUCTION

Myanmar is situated east of the oblique subduction zone of the Indian plate underneath the Eurasian plate. Plate convergence initiated during Aptian time (113–121 Ma; Cai et al., 2019) created a series of N-S-trending tectonic features, including mainly the Indo-Burman Ranges, the Central Basin, and the Sagaing fault (Fig. 1). The Indo-Burman Ranges are an accretionary wedge formed during the late Neogene and presently undergo dextral shear deformation (Maurin and Rangin, 2009). Bounded by the Kabaw fault on the west and the Sagaing fault on the east, the Central Basin is divided by the Wuntho-Popa volcanic arc into forearc and backarc basins. Belousov et al. (2018) reported eruptions in the Monywa and Popa areas (Fig. 1) along the Wuntho-Popa


arc at ca. 10,000 yr B.P. and ca. 8000 yr B.P., respectively, indicating ongoing volcanic activity. East of the Sagaing fault is the Mogok metamorphic belt, composed mainly of high-grade metamorphic rocks and granites (Searle et al., 2017).

Mantle flow patterns in the mantle wedge associated with oceanic subduction have been revealed by numerous seismic anisotropy studies (Long and Wirth, 2013). However, the mantle flow and more importantly the distribution of olivine fabric types above the subducting continental slab are still poorly understood. Seismic tomography and receiver functions reveal eastward-subducting Indian continental lithosphere with a dip angle of $\sim 25^\circ$ to a depth of at least 100 km beneath central Myanmar, between 22°N and 24°N (Zhang et al., 2021; Zheng et al., 2020). This region provides an ideal opportunity to study the distribution of olivine fabric types and flow patterns in the mantle wedge under continental subduction.

Seismic anisotropy in the upper mantle is caused largely by the lattice-preferred orienta-

tion of olivine. A-type olivine fabric, formed under water-poor conditions, aligns its fast axes parallel to the flow direction under large strain, causing faster shear waves polarized in the same direction (Karato et al., 2008). Therefore, the patterns of mantle flow and deformation can be inferred by obtaining the polarization orientation of the faster shear wave using the shear wave splitting (SWS) method. Additionally, B-type olivine fabric forms under conditions of high water content, low temperature, and high stress (Karato et al., 2008). Deformation experiments on strongly textured dunites have demonstrated the formation of an “apparent B-type” fabric when the pre-existing foliation aligns obliquely or parallel to the shortening direction (Boneh and Skemer, 2014; Boneh et al., 2015). Besides A- and B-type olivine fabrics, other fabric types include C- and E-type, which form under high-water-content, high-temperature, and low-stress conditions (Karato et al., 2008). However, under horizontal flow, C- and E-type olivine fabrics produce the same fast orientations as A-type fabric, while B-type fabric causes flow-perpendicular fast orientations.

The presence of B-type olivine fabric in the forearc mantle wedge and other types in the backarc has emerged as one of the plausible models to explain the 90° deflection of the fast orientations measured through local S splitting from the forearc to the backarc in some subduction zones (Long and Wirth, 2013). However, no previous studies have reported a 90° deflection of the fast orientations from local S waves within the forearc of any subduction zone. Numerous subduction zone models explain forearc mantle wedge anisotropy relying on a single type of

Yinshuang Ai  <https://orcid.org/0000-0001-6983-671X>

Stephen S. Gao  <https://orcid.org/0000-0001-7530-7128>

*ysai@mail.iggcas.ac.cn; sgao@mst.edu

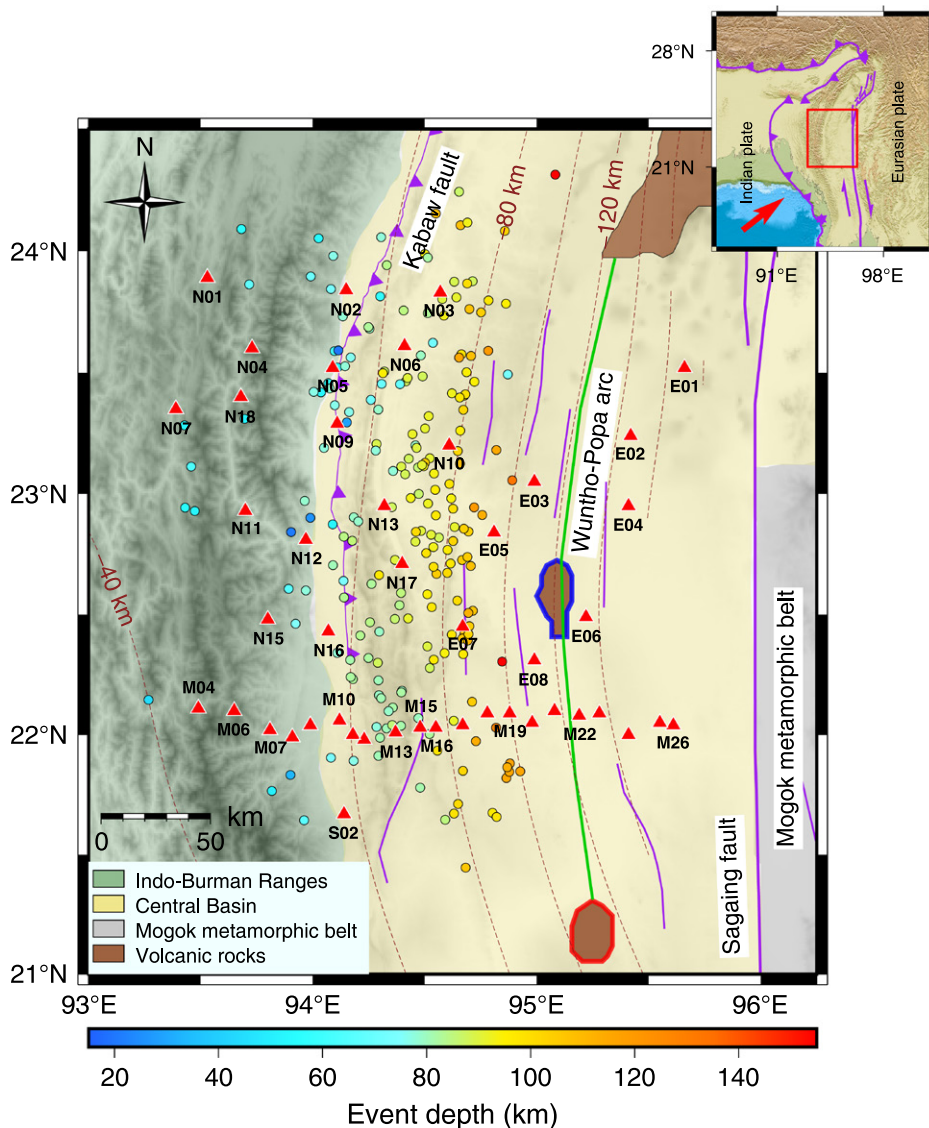


Figure 1. Tectonic setting of central Myanmar, showing seismic station and event distribution. Red triangles are seismic stations, and circles show event epicenters, color-coded by focal depth. Brown dashed lines mark slab contours (Hayes et al., 2018). Green line approximates the axis of the Wuntho-Popa volcanic arc (brown regions). Volcanic rocks in Popa and Monywa are outlined by thick red and blue lines, respectively. Red rectangle in the inset shows the study region. Red arrow in the inset shows the direction of absolute plate motion for the Indian plate (Argus et al., 2011), and purple curves show faults and plate boundaries.

olivine fabric with either trench-perpendicular or trench-parallel flow (Long and Wirth, 2013).

This study aims to provide seismic anisotropy constraints for understanding mantle flow patterns by considering various olivine fabric types in central Myanmar, an area underlain by the subducted Indian continental lithospheric slab.

RESULTS

The seismic data came from the China-Myanmar Geophysical Survey in the Myanmar Orogen (CMGSMO) array, which consisted of 46 stations (Fig. 1), operational from June 2016 to February 2018 (Mon et al., 2020). A total of 384 well-defined (quality A or B) local S splitting measurements were obtained (Fig. S1 in the

Supplemental Material¹) from 211 local events in central Myanmar (Figs. 1 and 2A). These measurements exhibit standard deviations of $<15^\circ$ for fast orientations and <0.1 s for splitting times. Because most earthquakes occurred within the subducting slab, the local S phases traversed through the slab, mantle wedge, and overriding crust (Fig. 2A), each potentially contributing to the observed splitting parameters.

¹Supplemental Material. Detailed descriptions of the data, methods, supplemental Figures S1–S9, and Table S1 (splitting parameters). Please visit <https://doi.org/10.1130/G51698.1/6173217/g51698.pdf> to access the supplemental material; contact editing@geosociety.org with any questions.

We observed higher spatial coherency of the splitting parameters (i.e., consistency among all splitting parameters in a given region) when placing the measurements at the mid-points between the stations and epicenters (Fig. 2B) than at individual stations or epicenters (Figs. S2b and S2c). The measurements show a unique pattern with trench-perpendicular fast orientations in a narrow band within the forearc sandwiched by two zones of trench-parallel fast orientations (Fig. 2B). Despite larger incidence angles causing more scattered fast orientations, the unique “sandwich” pattern persists across different incidence angle ranges (Fig. S3), and the splitting parameters do not vary significantly with the initial polarization direction (Fig. S4), suggesting that a single layer of anisotropy with a horizontal axis of symmetry is sufficient to explain the observations.

In the Indo-Burman Ranges, the dominant fast orientation is N-S, parallel to the strike of the Indo-Burman Ranges and slab contours (Fig. 2B). Along the northern and central segments of the Kabaw fault, fast orientations are mostly E-W. In the Central Basin, most fast orientations align with the strike of the slab contours. However, between the 80 and 100 km slab contours, fast orientations are dominantly perpendicular to the slab’s strike, except at the southernmost tip of the region delimited by these contours (Fig. 2B). The average splitting time for the entire study area is 0.35 ± 0.15 s. Some regions, like the SW corner of the study area and $\sim 23^\circ$ N on the Kabaw fault, exhibit longer splitting times, exceeding 0.4 s (Fig. 2C). In other areas with dense measurements, splitting times are close to the mean value and show no apparent correlation with focal depth (Fig. 2).

DISCUSSION

Contribution of the Crust and Subducting Slab

The crust’s contribution to observed anisotropy can be estimated by shear waves from local earthquakes within the crust. Near the Kabaw fault, SWS measurements with event depths shallower than the average Moho depth of 35 km (Zheng et al., 2020) show both fault-parallel (N-S) and fault-perpendicular (E-W) fast orientations (Fig. 2B). A common mechanism for the observed fast-orientation changes in the crust is stress-induced changes to microcrack geometry (Crampin and Peacock, 2008). The Kabaw fault is an E-dipping reverse fault, absorbing ~ 5 – 6 mm/yr of dextral motion (Pivnik et al., 1998; Steckler et al., 2016). Principal compressive stress directions from shallow earthquakes (<50 km) near the Kabaw fault (Mon et al., 2020) show both N-S and E-W orientations, explaining the observed N-S and E-W fast orientations, respectively.

The thin mantle wedge below the Indo-Burman Ranges (Zheng et al., 2020) indicates

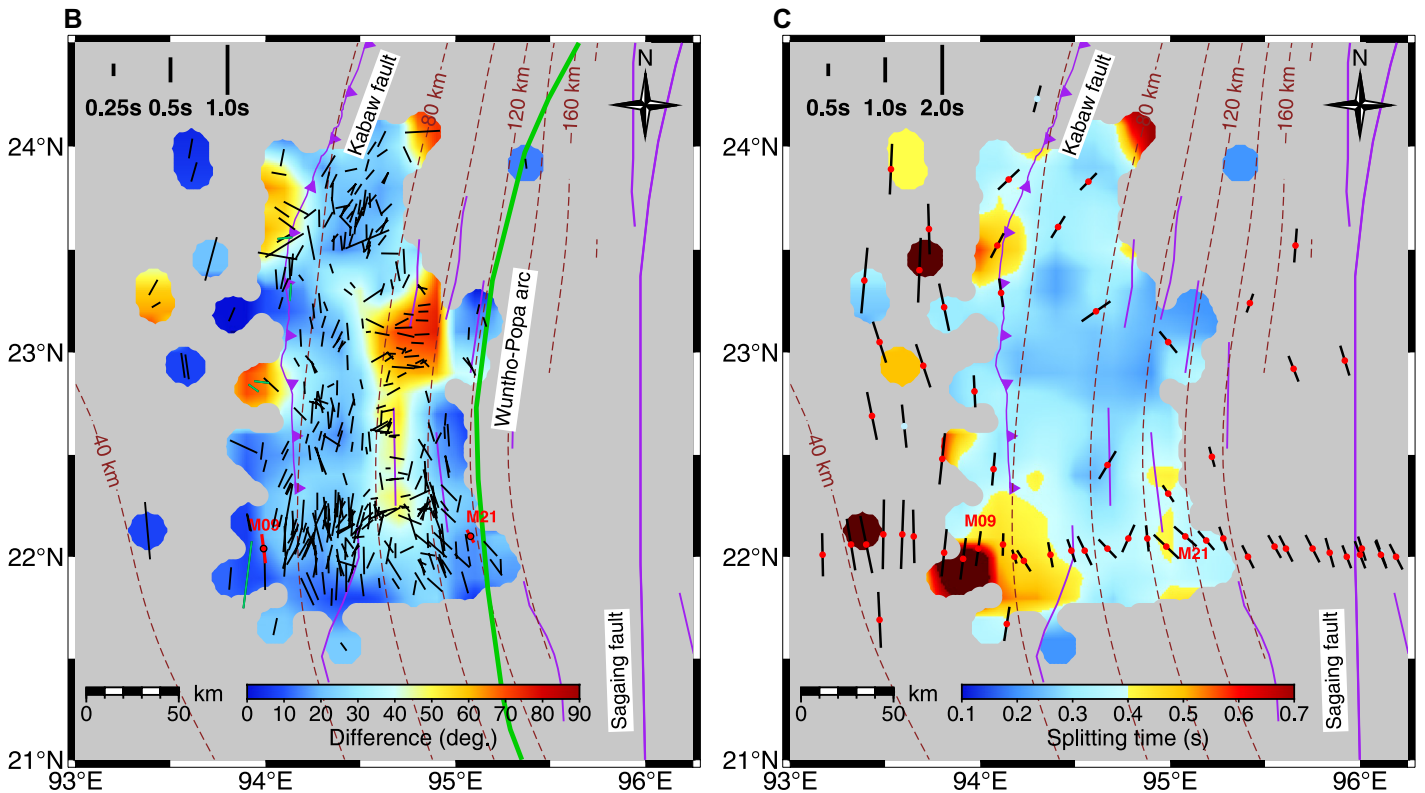
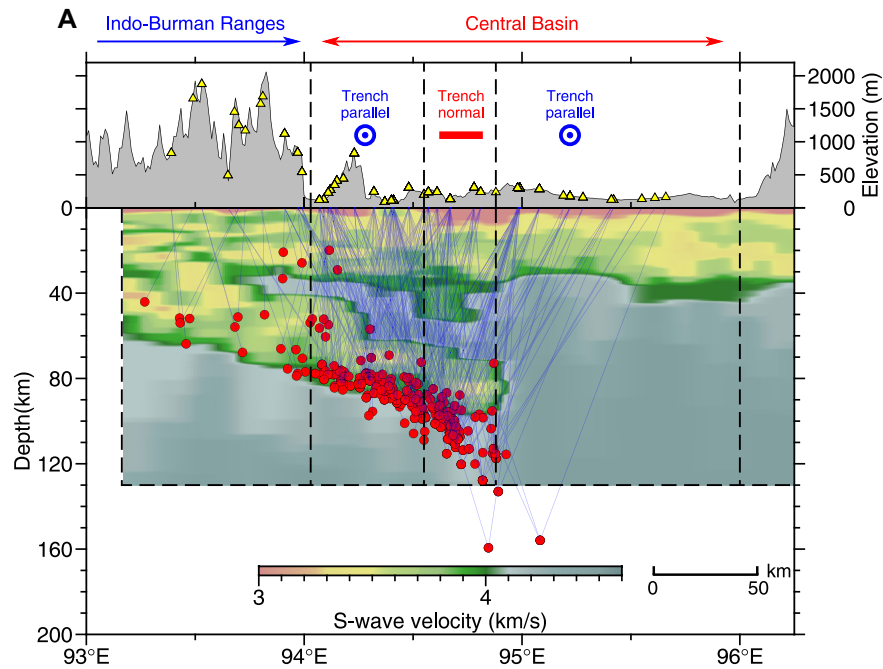


Figure 2. (A) Cross-section view displaying seismic stations (yellow triangles), local events (red dots), and ray paths (blue lines). Surface elevation and S-wave velocity along the 22°N latitude (Zheng et al., 2020) are shown in the upper and lower panels with vertical exaggerations of 31 and 1, respectively. (B) Local S-wave splitting measurements (black bars) at mid-points between epicenters and stations. Green bars show measurements with event depth <35 km. Background shows absolute difference between fast orientation and slab strike. Red bars show crustal anisotropy measurements at stations M09 (Fan et al., 2021) and M21. (C) Station-averaged teleseismic shear wave splitting measurements in black bars with red and light blue circles from Fan et al. (2021) and Liu et al. (2019), respectively, plotted on spatially smoothed local S-wave splitting times. For other symbols, see Figure 1.

that the splitting parameters reflect mainly the anisotropy of the subducting slab or the overlying accretionary wedge. The dominantly N-S fast orientations in the Indo-Burman Ranges, parallel to the strike of the orogen, agree with the

crustal anisotropy measurement at station M09 and teleseismic SWS measurements (Figs. 2B and 2C), supporting vertically coherent lithospheric deformation in the Indo-Burman Ranges (Fan et al., 2021).

Crustal anisotropy estimation in the Central Basin (Supplemental Material) is challenging due to the presence of a thick sediment layer (e.g., Zheng et al., 2020), resulting in reliable measurement at only one station (M21;

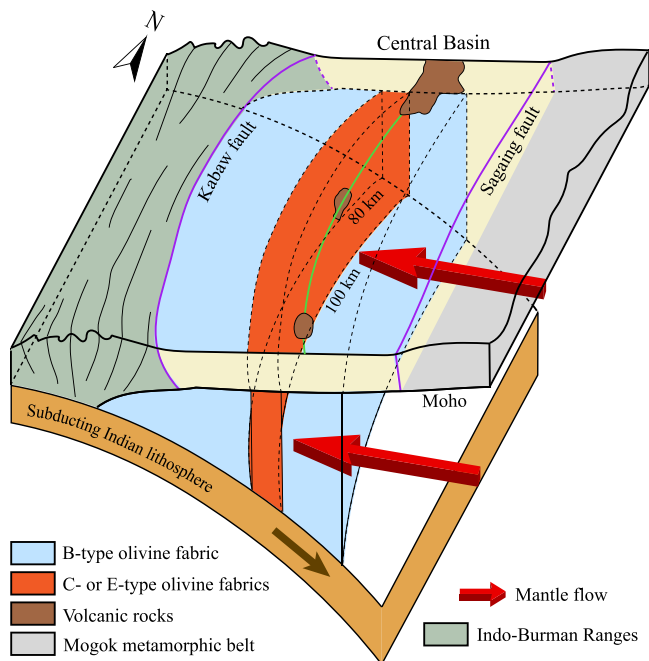


Figure 3. Summary of main findings in a three-dimensional schematic illustration. Green line represents the approximate axis of the Wuntho-Popa volcanic arc. Orange banded area between the 80 and 100 km slab contours indicates partial melting and C- or E-type olivine fabrics. Blue areas indicate B-type fabric. Red arrows indicate trench-perpendicular mantle flow toward the trench.

Fig. 2B; Fig. S5). The fast orientation (29.0°) of crustal anisotropy at station M21 is consistent with local S-wave measurements near the station, but the splitting time (0.29 s) is slightly smaller (Fig. 2B), suggesting additional anisotropic contributions below the crust. A series of N-S-striking dextral strike-slip faults with dominantly dextral strike-slip focal mechanisms in the Central Basin (Mon et al., 2020) would predict N-S fast orientations in the crust, inconsistent with the E-W fast orientations between the 80 and 100 km slab contours, except at the southernmost tip of the area where these orientations are observed (Fig. 2B). Additionally, weak coherence of the measurements placed at the stations (Fig. S2b) and at the epicenters (Fig. S2c) suggests that neither the near-station crust nor the subducting slab is the main source of anisotropy. Assuming anisotropy is preserved within the slab during subduction, as revealed in the subducted northern Philippine Sea plate (Liu et al., 2022), N-S fast orientations would appear in the Central Basin due to coherent deformation between the slab and overlying accretionary wedge beneath the Indo-Burman Ranges, inconsistent with the E-W fast orientations. Therefore, neither the crust nor the slab is likely the main contributor to the E-W-oriented anisotropy in the Central Basin.

Competing Flows in the Mantle Wedge

The mantle wedge is thus responsible for both E-W and N-S fast orientations in the Central Basin (Fig. 2B), supported by estimation of anisotropy depth using the spatial coherence method (Supplemental Material). Between 94.0°E and 94.5°E and east of 94.5°E , the optimal depths of the anisotropic layers are 40.0 km and 55.0 km, respectively (Fig. S6). Comparison

with the subducting slab's top interface depth of $\sim 60\text{--}120$ km (Hayes et al., 2018) and the average Moho depth of ~ 35 km (Zheng et al., 2020) reveals that the observed seismic anisotropy is mostly from the mantle wedge.

The mantle flow model by Fan et al. (2021) suggests coexistence of trench-parallel and corner flows induced by subduction and slab rollback in the mantle wedge beneath the Central Basin. Assuming A-type olivine fabric, fast orientation aligns parallel to flow direction. If corner flow prevailed, fast orientations would align perpendicular to the trench, and if trench-parallel flow prevailed, trench-parallel fast orientations would dominate. Although the observations can be explained by this model if corner flow between the 80 and 100 km slab contours is stronger than trench-parallel flow, the mechanisms behind corner flow's dominance in this narrow band remain unclear.

Transition of Olivine Fabric Types

Our favored model to explain the intriguing band of E-W fast orientations is a transition of olivine fabric types in the mantle wedge, which has not been previously proposed for the world's subduction zones. The wet mantle wedge with a water content of 0.25–0.54 wt% below central Myanmar (Sano et al., 2022) favors B-, C-, and E-type olivine fabrics (Jung et al., 2006; Karato et al., 2008; Katayama and Karato, 2006). Numerical simulations indicate that partial coupling between the subducting slab and the mantle wedge, compared to full coupling, leads to lower temperature and greater stress in the forearc mantle wedge, suitable for B-type olivine fabric (Kneller et al., 2005). The subduction zone thermal model by Wada and Wang (2009) supports the existence of a

cold forearc mantle due to decoupling between the slab and the overriding mantle. The Indian continental slab is older than most other oceanic slabs, which can lead to a colder overlying mantle wedge (e.g., Kincaid and Sacks, 1997). In addition, weak layers (subduction channels) on the surface of continental slabs (Zheng, 2012) may lead to decoupling or partial decoupling between the slab and the mantle. We propose that B-type olivine fabric is more widespread in the mantle wedge beneath the Central Basin under continental subduction relative to most mantle wedges above oceanic slabs and may even extend into the backarc (Fig. 3). The dominantly trench-parallel fast orientations in the Central Basin suggest trench-perpendicular corner flow (Figs. 2C and 3), produced by active subduction (Steckler et al., 2016) and slab rollback (Lee et al., 2016).

The anomalous E-W fast orientations between the 80 and 100 km slab contours on the western side of the volcanic arc can be explained by the presence of C- or E-type olivine fabrics (Figs. 2B and 3). The mantle wedge beneath the N-S-oriented band, dominated by E-W fast orientations, shows low S-wave velocity (Fig. 2A), interpreted as a zone of anomalously high partial melt due to slab dehydration lowering the melting point of overlying mantle minerals (Zheng et al., 2020). The presence of melts reduces mantle viscosity and shear stress (Kneller et al., 2005; Wada et al., 2008; Wiemer and Benoit, 1996), favoring C- or E-type olivine fabrics.

Another possible model is B-type olivine fabric between 80 and 100 km slab contours and A-type fabric elsewhere with trench-parallel flow. However, the wet mantle wedge (Sano et al., 2022) hinders A-type fabric. Additionally, we simulated splitting measurements for different olivine fabric types with various flow directions using the MSAT toolkit (Walker and Wookey, 2012). The residuals between observed and simulated results were notably larger when assuming A- and B-type fabrics with trench-parallel flow than involving B- and C- or E-type fabrics under trench-perpendicular flow (Figs. S7–S9, Supplemental Material). Consequently, we exclude A- and B-type fabrics with trench-parallel flow.

In conclusion, we propose a model illustrating the transition from B-type olivine fabric to C- or E-type fabric and back to B-type fabric from W to E in the forearc mantle wedge beneath central Myanmar (Fig. 3). The cold Indian continental slab, partially decoupled from the mantle, creates low-temperature and high-stress conditions west of the 80 km slab contour, promoting B-type fabric. Between the 80 and 100 km slab contours, partial melting induced by aqueous fluids favors C- or E-type fabric. As depth increases, the mantle-slab strength contrast diminishes, transitioning from decoupling

to coupling, promoting the reversion to B-type fabric (Wada et al., 2008).

Our findings have limitations: (1) an anisotropic transition zone between B- and C- or E-type olivine fabrics was not clearly observed due to the transition zone's weak anisotropy, limited station coverage, and complex anisotropic structure; and (2) the SWS method's poor vertical resolution hinders fully clarifying the contribution of A-type fabric in the lithosphere to the anisotropy signal. Future research using anisotropic surface waves may address these issues.

ACKNOWLEDGMENTS

We thank the CMGSMO seismic network for providing the data and editor R. Holdsworth and four anonymous reviewers for constructive comments. This study is supported by the National Natural Science Foundation of China (grants 42030309 and 42130308) and the U.S. National Science Foundation (awards 1830644 and 1919789). Seismic data can be accessed from <https://doi.org/10.12197/2023GA016>.

REFERENCES CITED

- Argus, D.F., Gordon, R.G., and DeMets, C., 2011, Geologically current motion of 56 plates relative to the no-net-rotation reference frame: *Geochemistry, Geophysics, Geosystems*, v. 12, Q11001, <https://doi.org/10.1029/2011GC003751>.
- Belousov, A., Belousova, M., Zaw, K., Streck, M.J., Bindeman, I., Meffre, S., and Vasconcelos, P., 2018, Holocene eruptions of Mt. Popa, Myanmar: Volcanological evidence of the ongoing subduction of Indian Plate along Arakan Trench: *Journal of Volcanology and Geothermal Research*, v. 360, p. 126–138, <https://doi.org/10.1016/j.jvolgeores.2018.06.010>.
- Boneh, Y., and Skemer, P., 2014, The effect of deformation history on the evolution of olivine CPO: *Earth and Planetary Science Letters*, v. 406, p. 213–222, <https://doi.org/10.1016/j.epsl.2014.09.018>.
- Boneh, Y., Morales, L.F.G., Kaminski, E., and Skemer, P., 2015, Modeling olivine CPO evolution with complex deformation histories: Implications for the interpretation of seismic anisotropy in the mantle: *Geochemistry, Geophysics, Geosystems*, v. 16, p. 3436–3455, <https://doi.org/10.1002/2015GC005964>.
- Cai, F., Ding, L., Zhang, Q., Orme, D.A., Wei, H., Li, J., Zhang, J., Zaw, T., and Sein, K., 2019, Initiation and evolution of forearc basins in the Central Myanmar Depression: *Geological Society of America Bulletin*, v. 132, p. 1066–1082, <https://doi.org/10.1130/B35301.1>.
- Crampin, S., and Peacock, S., 2008, A review of the current understanding of seismic shear-wave splitting in the Earth's crust and common fallacies in interpretation: *Wave Motion*, v. 45, p. 675–722, <https://doi.org/10.1016/j.wavemoti.2008.01.003>.
- Fan, E., He, Y., Ai, Y., Gao, S.S., Liu, K.H., Jiang, M., Hou, G., Mon, C.T., Thant, M., and Sein, K., 2021, Seismic anisotropy and mantle flow constrained by shear wave splitting in central Myanmar: *Journal of Geophysical Research: Solid Earth*, v. 126, <https://doi.org/10.1029/2021JB022144>.
- Hayes, G.P., Moore, G.L., Portner, D.E., Hearne, M., Flamme, H., Furtney, M., and Smoczyk, G.M., 2018, Slab2, a comprehensive subduction zone geometry model: *Science*, v. 362, p. 58–61, <https://doi.org/10.1126/science.aat4723>.
- Jung, H., Katayama, I., Jiang, Z., Hiraga, T., and Karato, S., 2006, Effect of water and stress on the lattice-preferred orientation of olivine: *Tectonophysics*, v. 421, p. 1–22, <https://doi.org/10.1016/j.tecto.2006.02.011>.
- Karato, S.-i., Jung, H., Katayama, I., and Skemer, P., 2008, Geodynamic significance of seismic anisotropy of the upper mantle: New insights from laboratory studies: *Annual Review of Earth and Planetary Sciences*, v. 36, p. 59–95, <https://doi.org/10.1146/annurev.earth.36.031207.124120>.
- Katayama, I., and Karato, S.-i., 2006, Effect of temperature on the B- to C-type olivine fabric transition and implication for flow pattern in subduction zones: *Physics of the Earth and Planetary Interiors*, v. 157, p. 33–45, <https://doi.org/10.1016/j.pepi.2006.03.005>.
- Kincaid, C., and Sacks, I.S., 1997, Thermal and dynamical evolution of the upper mantle in subduction zones: *Journal of Geophysical Research*, v. 102, p. 12,295–12,315, <https://doi.org/10.1029/96JB03553>.
- Kneller, E.A., van Keken, P.E., Karato, S.-i., and Park, J., 2005, B-type olivine fabric in the mantle wedge: Insights from high-resolution non-Newtonian subduction zone models: *Earth and Planetary Science Letters*, v. 237, p. 781–797, <https://doi.org/10.1016/j.epsl.2005.06.049>.
- Lee, H.-Y., Chung, S.-L., and Yang, H.-M., 2016, Late Cenozoic volcanism in central Myanmar: Geochemical characteristics and geodynamic significance: *Lithos*, v. 245, p. 174–190, <https://doi.org/10.1016/j.lithos.2015.09.018>.
- Liu, L., Gao, S.S., Liu, K.H., Li, S., Tong, S., and Kong, F., 2019, Toroidal mantle flow induced by slab subduction and rollback beneath the eastern Himalayan syntaxis and adjacent areas: *Geophysical Research Letters*, v. 46, p. 11,080–11,090, <https://doi.org/10.1029/2019GL084961>.
- Liu, Y., Xue, M., Guo, Z., and Zhu, A., 2022, Seismic anisotropy within the subducting northern Philippine Sea plate, SW Japan, using DONET seafloor observation network: *Geophysical Research Letters*, v. 49, <https://doi.org/10.1029/2021GL096516>.
- Long, M.D., and Wirth, E.A., 2013, Mantle flow in subduction systems: The mantle wedge flow field and implications for wedge processes: *Journal of Geophysical Research: Solid Earth*, v. 118, p. 583–606, <https://doi.org/10.1002/jgrb.50063>.
- Maurin, T., and Rangin, C., 2009, Structure and kinematics of the Indo-Burmese Wedge: Recent and fast growth of the outer wedge: *Tectonics*, v. 28, TC2010, <https://doi.org/10.1029/2008TC002276>.
- Mon, C.T., Gong, X., Wen, Y., Jiang, M., Chen, Q.-F., Zhang, M., Hou, G., Thant, M., Sein, K., and He, Y., 2020, Insight into major active faults in central Myanmar and the related geodynamic sources: *Geophysical Research Letters*, v. 47, <https://doi.org/10.1029/2019GL086236>.
- Pivnik, D.A., Nahm, J., Tucker, R.S., Smith, G.O., Nyein, K., Nyunt, M., and Maung, P.H., 1998, Polyphase deformation in a fore-arc/back-arc basin, Salin subbasin, Myanmar (Burma): *American Association of Petroleum Geologists Bulletin*, v. 82, p. 1837–1856, <https://doi.org/10.1306/1D9BD15F-172D-11D7-864500102C1865D>.
- Sano, T., et al., 2022, Petrogenesis of isotopically enriched Quaternary magma with adakitic affinity associated with subduction of old lithosphere beneath central Myanmar: *Scientific Reports*, v. 12, 3137, <https://doi.org/10.1038/s41598-022-07097-4>.
- Searle, M.P., Morley, C.K., Waters, D.J., Gardiner, N.J., Htun, U.K., Than Than, N., and Robb, L.J., 2017, Tectonic and metamorphic evolution of the Mogok Metamorphic and Jade Mines belts and ophiolitic terranes of Burma (Myanmar), in Barber, A.J., et al., eds., *Myanmar: Geology, Resources and Tectonics*: Geological Society, London, Memoir 48, p. 261–293, <https://doi.org/10.1144/M48.12>.
- Steckler, M.S., Mondal, D.R., Akhter, S.H., Seeber, L., Feng, L., Gale, J., Hill, E.M., and Howe, M., 2016, Locked and loading megathrust linked to active subduction beneath the Indo-Burman Ranges: *Nature Geoscience*, v. 9, p. 615–618, <https://doi.org/10.1038/ngeo2760>.
- Wada, I., and Wang, K., 2009, Common depth of slab-mantle decoupling: Reconciling diversity and uniformity of subduction zones: *Geochemistry, Geophysics, Geosystems*, v. 10, Q10009, <https://doi.org/10.1029/2009GC002570>.
- Wada, I., Wang, K., He, J., and Hyndman, R.D., 2008, Weakening of the subduction interface and its effects on surface heat flow, slab dehydration, and mantle wedge serpentinization: *Journal of Geophysical Research*, v. 113, B04402, <https://doi.org/10.1029/2007JB005190>.
- Walker, A.M., and Wookey, J., 2012, MSAT—A new toolkit for the analysis of elastic and seismic anisotropy: *Computers & Geosciences*, v. 49, p. 81–90, <https://doi.org/10.1016/j.cageo.2012.05.031>.
- Wiemer, S., and Benoit, J.P., 1996, Mapping the B-value anomaly at 100 km depth in the Alaska and New Zealand Subduction Zones: *Geophysical Research Letters*, v. 23, p. 1557–1560, <https://doi.org/10.1029/96GL01233>.
- Zhang, G., He, Y., Ai, Y., Jiang, M., Mon, C.T., Hou, G., Thant, M., and Sein, K., 2021, Indian continental lithosphere and related volcanism beneath Myanmar: Constraints from local earthquake tomography: *Earth and Planetary Science Letters*, v. 567, <https://doi.org/10.1016/j.epsl.2021.116987>.
- Zheng, T., He, Y., Ding, L., Jiang, M., Ai, Y., Mon, C.T., Hou, G., Sein, K., and Thant, M., 2020, Direct structural evidence of Indian continental subduction beneath Myanmar: *Nature Communications*, v. 11, p. 1944, <https://doi.org/10.1038/s41467-020-15746-3>.
- Zheng, Y.-F., 2012, Metamorphic chemical geodynamics in continental subduction zones: *Chemical Geology*, v. 328, p. 5–48, <https://doi.org/10.1016/j.chemgeo.2012.02.005>.

Printed in the USA